Inorg. Chem. **2009**, *48*, 2593−2604

Electrochemical and Chemical Oxidation of $[Pt_2(\mu\text{-pyrophosphite})_4]^{4-}$ Revisited: Characterization of a Nitrosyl Derivative, $[Pt_2(\mu\text{-pyrophosphite})_4(NO)]^{3-}$

Martin A. Bennett,[†] Suresh K. Bhargava,[*,‡] Alan M. Bond,[*,§] Vipul Bansal,[‡] Craig M. Forsyth,[§] Si-Xuan Guo,[§] and Steven H. Privér[‡]

Research School of Chemistry, Australian National University, Canberra, ACT 0200, Australia, School of Applied Sciences (Applied Chemistry), RMIT University, GPO Box 2476V, Melbourne, Victoria 3001, Australia., and School of Chemistry, Monash University, Clayton, Victoria 3800, Australia

Received November 18, 2008

Electrochemical studies of the salts $[cat]_4[Pt_2(\mu\text{-pop})_4]$ ($cat^+ = Bu_4N^+$ or PPN^+ $[Ph_3P{=}N{=}PPh_3]^+$; pop = pyrophosphite, $[P_2O_5H_2]^{2-}$) have been carried out in dichloromethane. In agreement with published studies of $K_4[Pt_2(\mu\text{-pop})_4]$ in water and $[Ph_4As]_4[Pt_2(\mu\text{-pop})_4]$ in acetonitrile, the $[Pt_2(\mu\text{-pop})_4]^{4-}$ anion is found to undergo an initial one-electron oxidation under conditions of cyclic voltammetry to a short-lived trianion, $[Pt_2(\mu\text{-pop})_4]^{3-}$. However, in the more weakly coordinating solvent dichloromethane, $[Pt_2(\mu\text{-pop})_4]^{3-}$ appears to undergo oligomerization instead of solvent-induced disproportionation; thus the overall process remains a one-electron reaction rather than an overall two-electron oxidative addition process, even under long time-scale, bulk electrolysis conditions. Chemical oxidation of $[cat]_4[Pt_2(\mu\text{-pop})_4]$ with $[NO][BF_4]$ or $AgBF_4$ gives mainly a dark, insoluble, ill-defined solid that appears to contain Pt(III) according to X-ray photoelectron spectroscopy (XPS). In the case of $[NO][BF_4]$, a second reaction product, an orange solid, has been identified as a nitrosyl complex, $[cat]_3[Pt_2(\mu\text{-pop})_4(NO)]$. The X-ray structure of the PPN^+ salt shows the anion to consist of the usual lantern-shaped $Pt_2(\mu\text{-pop})_4$ framework with an unusually large Pt−Pt separation [2.8375(6) Å]; one of the platinum atoms carries a bent nitrosyl group [r(N−O) = 1.111(15) Å; ∠(Pt−N−O) = 118.1(12)°] occupying an axial position. The nitrosyl group migrates rapidly on the ^{31}P NMR time-scale between the metal atoms at room temperature but the motion is slow enough at 183 K that the expected two pairs of inequivalent phosphorus nuclei can be observed. The X-ray photoelectron (XP) spectrum of the nitrosyl-containing anion confirms the presence of two inequivalent platinum atoms whose $4f_{7/2}$ binding energies are in the ranges expected for Pt(II) and Pt(III); an alternative interpretation is that the second platinum atom has a formal oxidation number of +4 and that its binding energy is modified by the strongly σ-donating NO^- ligand. Reduction of $[Pt_2(\mu\text{-pop})_4X_2]^{4-}$ (X = Cl, Br, I) in dichloromethane corresponds to a chemically reversible, electrochemically irreversible two-electron process involving loss of halide and formation of $[Pt_2(\mu\text{-pop})_4]^{4-}$, as is the case in more strongly coordinating solvents.

Introduction

The chemistry and photophysics of the lantern-shaped diplatinum(II) anion $[Pt_2(\mu\text{-pop})_4]^{4-}$ (**1**) (pop = pyrophosphite, $[P_2O_5H_2]^{2-}$) (Figure 1) have attracted much interest since the preparation of the potassium salt and the discovery of its intense, long-lived luminescence in aqueous solution;[1,2] the early history has been reviewed.[3−5]

According to the simple molecular orbital (MO) treatment developed for binuclear d^7-d^7 and d^8-d^8 metal complexes,[6] the ground-state of $[Pt_2(\mu\text{-pop})_4]^{4-}$ has an electronic config-

* To whom correspondence should be addressed. E-mail: suresh.bhargava@rmit.edu.au (S.K.B.), alan.bond@sci.monash.edu.au (A.M.B.).
† Australian National University.
‡ RMIT University.
§ Monash University.

(1) Sperline, R. M.; Dickson, M. K.; Roundhill, D. M. *J. Chem. Soc., Chem. Commun.* **1977**, 62.
(2) Filomenia Dos Remedios Pinto, M. A.; Sadler, P. J.; Neidle, S.; Sanderson, M. R.; Subbiah, A.; Kuroda, R. *J. Chem. Soc., Chem. Commun.* **1980**, 13.

10.1021/ic802213v CCC: $40.75
Published on Web 02/18/2009

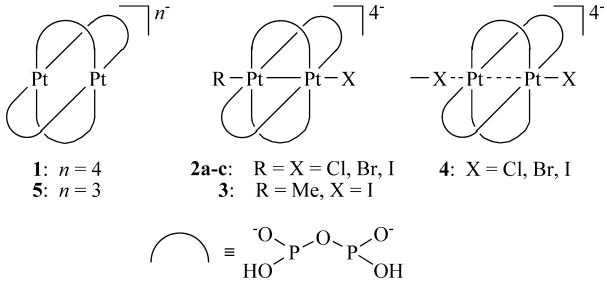

Figure 1. μ-Pyrophosphite complexes of platinum.

uration $(d\sigma)^2(d\sigma^*)^2$, with a bond order of zero, and the photophysical properties are associated with a low-lying triplet state derived from the $(d\sigma)^2(d\sigma^*)(p\sigma)$ configuration. The anion readily undergoes two-electron oxidative additions with halogen (X_2) or alkyl halides (RX) to give diplatinum(III) (d^7-d^7) complexes $[Pt_2(\mu\text{-pop})_4X_2]^{4-}$ [X = Cl (**2a**), Br (**2b**), I (**2c**)] and $[Pt_2(\mu\text{-pop})_4X(R)]^{4-}$ (**3**), respectively.[7−11] The former are also obtained by addition of one-electron oxidants to, or by electrochemical oxidation of, $[Pt_2(\mu\text{-pop})_4]^{4-}$ in the presence of halide ion.[12−14] In these reactions, the two $d\sigma^*$ electrons of $[Pt_2(\mu\text{-pop})_4]^{4-}$ are removed, and the resulting anion contains a metal−metal bond of bond order 1 between the two d^7 metal centers.

Mixed-valent Pt(II)−Pt(III) complexes containing the anions $[Pt_2(\mu\text{-pop})_4X]^{4-}$ (**4**) can also be isolated, either by partial oxidation of $[Pt_2(\mu\text{-pop})_4]^{4-}$ or by comproportionation between $[Pt_2(\mu\text{-pop})_4]^{4-}$ and $[Pt_2(\mu\text{-pop})_4X_2]^{4-}$.[7,8,12,15] The latter reaction is reversed rapidly in aqueous solution and there is no evidence for the existence of the discrete anions **4** in solution; in the solid state the compounds consist of infinite linear chains of $Pt_2(\mu\text{-pop})_4$ units bridged by halide ions,[8,12,16−18] and they behave as one-dimensional (1-D) semiconductors whose spectroscopic, magnetic, conducting, and other physical properties have been the focus of recent attention.[19−21]

The one-electron oxidized product $[Pt_2(\mu\text{-pop})_4]^{3-}$ (**5**) (eq 1), or more plausibly, solvated $[Pt_2(\mu\text{-pop})_4(\text{solvent})]^{3-}$ or halogenated $[Pt_2(\mu\text{-pop})_4X]^{4-}$ intermediates, as appropriate, have been implicated in the thermal reaction of $[Pt_2(\mu\text{-pop})_4]^{4-}$ with one-electron oxidants and with H_2O_2,[10,13] and in the photoinduced reaction of $[Pt_2(\mu\text{-pop})_4]^{4-}$ with aryl halides.[22,23] The anion $[Pt_2(\mu\text{-pop})_4]^{3-}$ has been detected directly both in the photoionization of $[Pt_2(\mu\text{-pop})_4]^{4-}$ in aqueous solution and in the reaction of $[Pt_2(\mu\text{-pop})_4]^{4-}$ with hydroxyl radicals,[24,25] and decays according to a second-order pathway (eq 2) with a rate constant of 6.7×10^8 M^{-1} s^{-1}. Finally, cyclic voltammetry of $[Pt_2(\mu\text{-pop})_4]^{4-}$, in the form of its Bu_4N^+ and Ph_4As^+ salts in acetonitrile in the absence of halide ion, was reported[14] to show partial chemical reversibility at a scan rate of 1000 V s^{-1}, presumably on account of formation of $[Pt_2(\mu\text{-pop})_4(NCCH_3)]^{3-}$ stabilized against disproportionation by axial coordination of the solvent. Clearly the role of the solvent can be critical in determining the reaction pathway in the oxidation of $[Pt_2(\mu\text{-pop})_4]^{4-}$.

$$[Pt_2(\mu\text{-pop})_4]^{4-} \rightarrow \underset{\mathbf{5}}{[Pt_2(\mu\text{-pop})_4]^{3-}} + e^- \quad (1)$$

$$2[Pt_2(\mu\text{-pop})_4]^{3-} \xrightarrow{H_2O} [Pt_2(\mu\text{-pop})_4]^{4-} + [Pt_2(\mu\text{-pop})_4(H_2O)_2]^{2-} \quad (2)$$

The neutral diplatinum(II) complexes $[Pt_2(\mu\text{-ArNCHNAr})_4]$ (Ar = Ph, *p*-tol)[26] and $[Pt_2(\mu\text{-}C_6H_3\text{-5-Me-2-As}Ph_2)_4]$,[27] which contain, respectively, diarylformamidinato and 5-tolyl-2-diphenylarsino bridging ligands, resemble $[Pt_2(\mu\text{-pop})_4]^{4-}$ in having lantern or paddle-wheel structures. Under voltammetric conditions, they undergo a reversible one-electron oxidation process in dichloromethane to give the corresponding platinum(II)−platinum(III) cations, which can be isolated by chemical oxidation as PF_6^- salts and contain a Pt−Pt bond of order 0.5.[28,29] These observations prompted us to extend the earlier study[14] on the electrochemical oxidation of $[Pt_2(\mu\text{-pop})_4]^{4-}$ to the poorly coordi-

(3) Zipp, A. P. *Coord. Chem. Rev.* **1988**, *84*, 47.
(4) Roundhill, D. M.; Gray, H. B.; Che, C.-M. *Acc. Chem. Res.* **1989**, *22*, 55.
(5) Murillo, C. A. In *Multiple Bonds Between Metal Atoms*, 3rd ed.; Cotton, F. A., Murillo, C. A., Walton, R. M., Eds.; Springer: New York, 2005; Chapter 14, pp 644, 658.
(6) Mann, K. R.; Gordon, J. G., II.; Gray, H. B. *J. Am. Chem. Soc.* **1975**, *97*, 3553.
(7) Che, C.-M.; Schaefer, W. P.; Gray, H. B.; Dickson, M. K.; Stein, P. B.; Roundhill, D. M. *J. Am. Chem. Soc.* **1982**, *104*, 4253.
(8) Che, C.-M.; Herbstein, F. M.; Schaefer, W. P.; Marsh, R. E.; Gray, H. B. *J. Am. Chem. Soc.* **1983**, *105*, 4604.
(9) Che, C.-M.; Mak, T. C.; Gray, H. B. *Inorg. Chem.* **1984**, *23*, 4386.
(10) Che, C.-M.; Butler, L. G.; Grunthaner, P. J.; Gray, H. B. *Inorg. Chem.* **1985**, *24*, 4662.
(11) Alexander, K. A.; Bryan, S. A.; Fronczek, F. R.; Fultz, W. C.; Rheingold, A. L.; Roundhill, D. M.; Stein, P.; Watkins, S. F. *Inorg. Chem.* **1985**, *24*, 2803.
(12) Clark, R. J. H.; Kurmoo, M.; Dawes, H. M.; Hursthouse, M. B. *Inorg. Chem.* **1986**, *25*, 409.
(13) Bryan, S. A.; Dickson, M. K.; Roundhill, D. M. *J. Am. Chem. Soc.* **1984**, *106*, 1882.
(14) Bryan, S. A.; Schmehl, R. H.; Roundhill, D. M. *J. Am. Chem. Soc.* **1986**, *108*, 5408.
(15) Kurmoo, M.; Clark, R. J. H. *Inorg. Chem.* **1985**, *24*, 4420.
(16) Butler, L. G.; Zietlow, M. H.; Che, C.-M.; Schaefer, W. P.; Sridhar, S.; Grunthaner, P. J.; Swanson, B. I.; Clark, R. J. H.; Gray, H. B. *J. Am. Chem. Soc.* **1988**, *110*, 1155.
(17) Jin, S.; Ito, T.; Toriumi, K.; Yamashita, M. *Acta Crystallogr., Sect. C* **1989**, *45*, 1415.
(18) Yamashita, M.; Toriumi, K. *Inorg. Chim. Acta* **1990**, *178*, 143.
(19) Yamashita, M.; Miya, S.; Kawashima, T.; Manabe, T.; Sonoyama, T.; Kitagawa, H.; Mitani, T.; Okamoto, H.; Ikeda, R. *J. Am. Chem. Soc.* **1999**, *121*, 2321.
(20) Ikeda, R. *Bull. Chem. Soc. Jpn.* **2004**, *77*, 1075; and references cited therein.
(21) Mastuzaki, H.; Kishida, H.; Okamoto, H.; Takizawa, K.; Matsunaga, S.; Takaishi, S.; Miyasaka, H.; Sugiura, K.; Yamashita, M. *Angew. Chem., Int. Ed.* **2005**, *44*, 3240.
(22) Roundhill, D. M. *J. Am. Chem. Soc.* **1985**, *107*, 4354.
(23) Roundhill, D. M.; Dickson, M. K.; Atherton, S. J. *J. Organomet. Chem.* **1987**, *335*, 413.
(24) Roundhill, D. M.; Atherton, S. J. *J. Am. Chem. Soc.* **1986**, *108*, 6829.
(25) Cho, K. C.; Che, C.-M. *Chem. Phys. Lett.* **1986**, *124*, 313.
(26) Cotton, F. A.; Matonic, J. H.; Murillo, C. A. *Inorg. Chem.* **1996**, *35*, 498.
(27) Bennett, M. A.; Bhargava, S. K.; Bond, A. M.; Edwards, A. J.; Guo, S.-X.; Privér, S. H.; Rae, A. D.; Willis, A. C. *Inorg. Chem.* **2004**, *43*, 7752.
(28) Cotton, F. A.; Matonic, J. H.; Murillo, C. A. *Inorg. Chim. Acta* **1997**, *264*, 61.
(29) Bennett, M. A.; Bhargava, S. K.; Boas, J. F.; Boeré, R. T.; Bond, A. M.; Edwards, A. J.; Guo, S.-X.; Hammerl, A.; Pilbrow, J. R.; Privér, S. H.; Schwerdtfeger, P. *Inorg. Chem.* **2005**, *44*, 2472.

nating solvent dichloromethane in an effort to obtain additional evidence for the formation of $[Pt_2(\mu\text{-pop})_4]^{3-}$ and its reaction pathways under these conditions. We have also investigated one-electron chemical oxidation of $[Pt_2(\mu\text{-pop})_4]^{4-}$ in CH_2Cl_2 with $AgBF_4$ and $[NO][BF_4]$; the latter reagent has led to the formation of an unprecedented terminal nitrosyl complex containing the $Pt_2(\mu\text{-pop})_4$ unit. Finally, to confirm several aspects of the oxidative electrochemistry, reduction of $[Pt_2(\mu\text{-pop})_4X_2]^{4-}$ also has been studied in dichloromethane for the first time.

Results

Oxidative Electrochemistry of $[Pt_2(\mu\text{-pop})_4]^{4-}$ in Dichloromethane. Since the parent compound $K_4[Pt_2(\mu\text{-pop})_4]$ is insoluble in CH_2Cl_2, the more soluble salts containing the cations tetrabutylammonium and bis(triphenylphosphine)-iminium, $[Ph_3P{=}N{=}PPh_3]^+$, abbreviated as PPN^+, were employed in this solvent. These salts were obtained by treatment of an aqueous solution of the potassium salt with an excess of $[Bu_4N]Cl$ and [PPN]Cl, respectively. The voltammetric responses of 0.2 mM and 1.0 mM solutions of the Bu_4N^+ and PPN^+ salts in CH_2Cl_2 containing 0.1 M $[Bu_4N][PF_6]$ were indistinguishable, so only the behavior of the PPN^+ salt is reported. No processes were observed for the reduction of $[Pt_2(\mu\text{-pop})_4]^{4-}$ in dichloromethane, either at room temperature (20 ± 2 °C) or at low temperature (75 ± 2 °C). All potentials in the following discussion are quoted relative to the ferrocene/ferrocenium (Fc/Fc^+) couple.

Under conditions of cyclic voltammetry at a glassy carbon macrodisk electrode, two major oxidation processes for $[Pt_2(\mu\text{-pop})_4]^{4-}$ with approximately equal peak heights were observed at about +200 mV (partially reversible) and +850 mV (irreversible) prior to the onset of the solvent oxidation at about +1200 mV. A small oxidation response at about +500 mV (Figure 2) at a glassy carbon electrode was more prominent on gold and platinum electrodes. Since its profile also depended on the treatment of the electrode surface, this response is probably associated with adsorption on the electrode surface. The first oxidation process forms the focus of this study. Panels a−d of Figure 3 show cyclic voltammograms for this process at room temperature as a function of scan rate from a 1.0 mM solution of $[PPN]_4[Pt_2(\mu\text{-pop})_4]$ in CH_2Cl_2 containing 0.1 M $[Bu_4N][PF_6]$ as supporting electrolyte. At 100 mV s^{-1} or less, a reverse peak associated with product reduction was barely detectable and, although it became more prominent with increasing scan rate, full chemical reversibility was not achieved at a scan rate of 5 V s^{-1} [Figure 3d] or at 200 V s^{-1} using a carbon fiber microelectrode. A significant decrease in oxidation peak current was also detected on repetitive scanning of the potential. These results indicate that complex homogeneous reactions follow the electron transfer process.

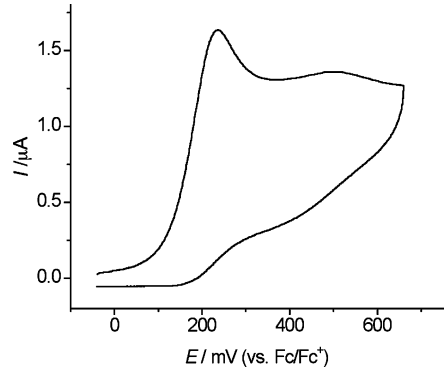

Figure 2. Cyclic voltammogram for the initial process for oxidation of 1.0 mM $[Pt_2(\mu\text{-pop})_4]^{4-}$ in CH_2Cl_2 (0.1 M $[Bu_4N][PF_6]$) at a glassy carbon electrode. Temperature = 20 °C, scan rate = 100 mV s^{-1}.

The cyclic voltammetric results obtained from solutions of $[PPN]_4[Pt_2(\mu\text{-pop})_4]$ (1.0 mM and 0.1 mM) in CH_2Cl_2 containing 0.02 M $[Bu_4N][PF_6]$ at −75 °C differed from those at room temperature. For both concentrations, the reverse peak was now more prominent at slow scan rates but again never became fully reversible in the chemical sense at higher scan rates (Supporting Information, Figure S1). Thus, fully reversible behavior was not obtained, even at low temperature, confirming that the initial oxidation step in dichloromethane involves complex chemistry coupled to the electron transfer reaction.

The cyclic voltammetric behavior of 1.0 mM and 0.2 mM solutions of $[PPN]_4[Pt_2(\mu\text{-pop})_4]$ in CH_2Cl_2 containing either $[Bu_4N][BArF_{24}]$ ($[BArF_{24}]^- = [B\{3,5\text{-}(CF_3)_2C_6H_3\}_4]^-$) or $[Bu_4N][B(C_6F_5)_4]$ at 0.05 M concentration as the supporting electrolyte was identical with that reported for $[Bu_4N][PF_6]$, both at 20 °C and −75 °C. The $[BArF_{24}]^-$ and $[B(C_6F_5)_4]^-$ anions are poor nucleophiles in solvents of low polarity.[30] The results imply that $[Bu_4N][PF_6]$ is an essentially innocent electrolyte with respect to electron transfer and coupled chemical reactions.

It is difficult to establish by cyclic voltammetry the number of electrons transferred in the first oxidation process under transient conditions when complex reactions occur subsequently. This parameter is more reliably determined from steady-state experiments at a rotating disk electrode (RDE). Measurements at a glassy RDE on a 1.0 mM solution of $[PPN]_4[Pt_2(\mu\text{-pop})_4]$ in CH_2Cl_2 showed a linear dependence of the limiting current on the square root of the angular frequency of rotation. The diffusion coefficient derived from the Levich equation[31] was 4.0 ± 0.2 × 10^{-6} cm^2 s^{-1}, assuming the oxidation to be an overall one-electron process. This value is similar to that obtained for the lantern dimer $[Pt_2(\mu\text{-}C_6H_3\text{-}5\text{-Me-}2\text{-}AsPh_2)_4]$ in dichloromethane (5.2 ± 0.2 × 10^{-6} cm^2 s^{-1}).[29] The half-wave potential of +203 mV for the first oxidation process at the RDE (corrected for uncompensated resistance) was almost identical to the midpoint potentials (+201 mV) calculated from cyclic voltammograms obtained at scan rates of 2 or 5 V s^{-1}. Finally, the assignment as a one-electron process was supported by noting that the limiting current magnitude per unit concentration under RDE conditions is close to half of that for the known overall two-electron reduction of $[Pt_2(\mu\text{-pop})_4X_2]^{4-}$ (X = Cl, Br, I) in dichloromethane to $[Pt_2(\mu\text{-pop})_4]^{4-}$ (see later). All these data are consistent with the overall charge transfer process being a one-electron process (eq 1), but with complex accompanying homogeneous chemistry.

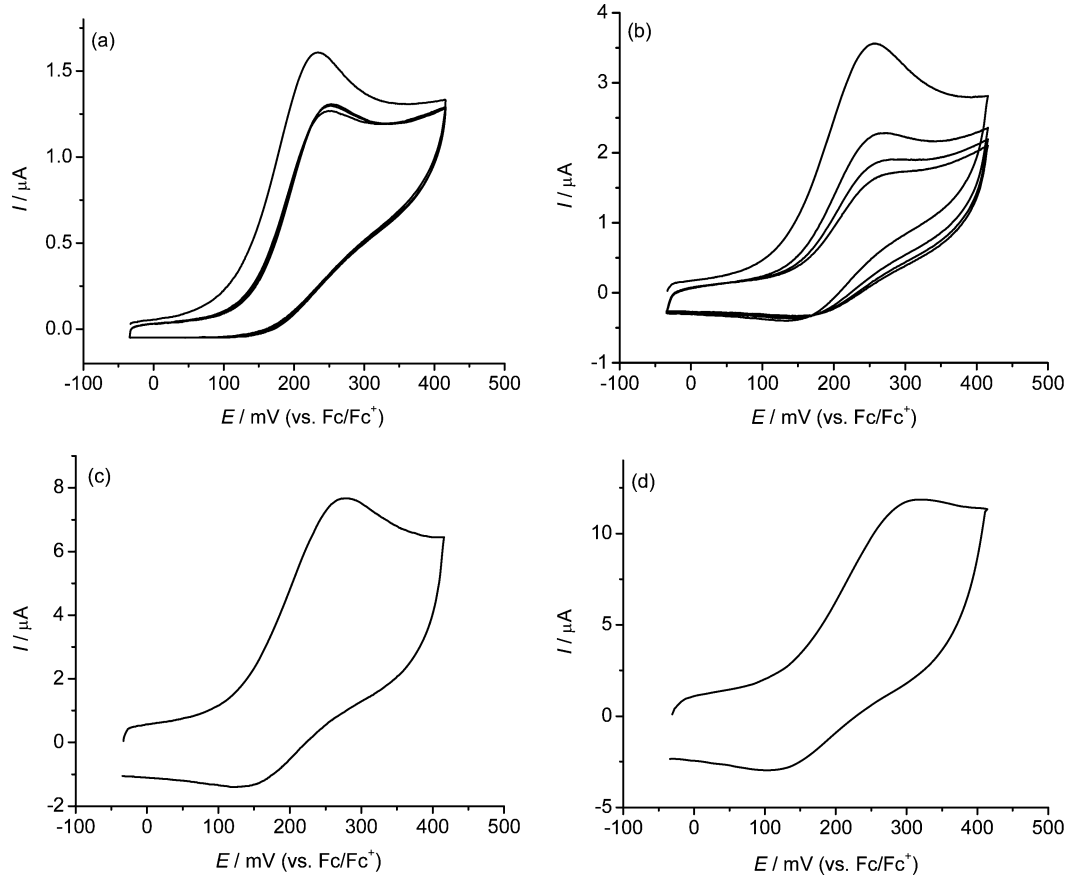

Figure 3. Cyclic voltammograms of 1.0 mM $[Pt_2(\mu\text{-pop})_4]^{4-}$ in CH_2Cl_2 (0.1 M $[Bu_4N][PF_6]$) as a function of scan rate for the first oxidation process at a glassy carbon electrode at 20 °C. (a) 100 mV s^{-1}, (b) 500 mV s^{-1}, (c) 2000 mV s^{-1}, and (d) 5000 mV s^{-1}.

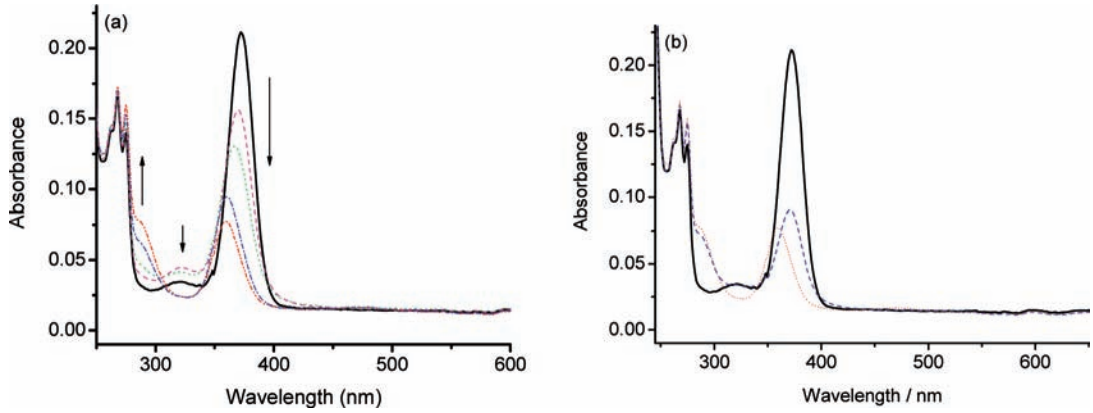

Figure 4. (a) UV−visible spectra of 0.5 mM $[Pt_2(\mu\text{-pop})_4]^{4-}$ obtained in CH_2Cl_2 in a spectroelectrochemical experiment during the course of oxidative electrolysis +300 mV. Before oxidation (black solid line), 5th cycle (purple dashed line), 10th cycle (green dotted line), 39th cycle (blue dash-dot line) and 78th cycle (red dash-dot-dot line). (b) Comparison of spectra of 0.5 mM $[Pt_2(\mu\text{-pop})_4]^{4-}$ in CH_2Cl_2 before electrolysis (black), after oxidation at +300 mV (red) and after reduction of the oxidized species (blue) at 0 mV.

Simulations of mechanisms involving a one-electron oxidation followed by product oligomerization exhibited qualitative agreement with experimental cyclic voltammograms. However, simulations with a unique set of parameters could not be matched quantitatively over all scan rates and concentrations studied, probably for two reasons: (a) no allowance was made for the experimentally detected adsorption, and (b) several non-first order reactions, whose rates are concentration-dependent, may occur after the initial electron-transfer.

UV−visible Spectroelectrochemistry. During the course of oxidative electrolysis of a solution of 0.5 mM $[PPN]_4[Pt_2(\mu\text{-pop})_4]$ in CH_2Cl_2 at +300 mV using a Pt gauze working electrode in a thin layer configuration, the color changed from pale greenish-yellow to light orange. As shown in Figure 4a, this change was associated with a decrease in intensity of the band at 372 nm and a shift of the maximum wavelength in this region to 363 nm; the intensity of the band due to $[Pt_2(\mu\text{-pop})_4]^{4-}$ at 322 nm ultimately also decreased. A new band at 287 nm formed slowly as the

oxidation proceeded, consistent with formation of a small concentration of $[Pt_2(\mu\text{-pop})_4Cl_2]^{4-}$ (see spectral data below), the Cl^- presumably being derived from the dichloromethane solvent. However, there were no isosbestic points, indicating that one or more intermediates had been generated before the final product had been formed. Bands at 310 and 248 nm, which have been assigned to $[Pt_2(\mu\text{-pop})_4]^{3-}$ and $[Pt_2(\mu\text{-pop})_4]^{2-}$, respectively, in water[24] were not observed, and there was no band in the near-IR region that might have indicated the presence of a mixed-valent species. Reductive electrolysis of the oxidized solution at a potential of 0 mV led to partial recovery of the absorbances at 372 and 322 nm, but the absorbance at 372 nm after the oxidation−reduction cycle was less than half of its initial value. The band at 287 nm remained unaltered, as expected, since this is assigned to $[Pt_2(\mu\text{-pop})_4Cl_2]^{4-}$ which cannot be reduced at 0 mV (see later).

Clearly, the oxidation of $[Pt_2(\mu\text{-pop})_4]^{4-}$ in the weakly coordinating solvent dichloromethane is complex. The spectroelectrochemical studies of 0.5 mM $[Pt_2(\mu\text{-pop})_4]^{4-}$ were therefore also carried out in the presence of halide to ascertain if the presence of a coordinating ligand altered the reaction. In the presence of 1 equiv or more of Cl^-, two isosbestic points were observed when the spectra were collected at various stages during the course of oxidative electrolysis at +300 mV. The absorption band at 372 nm decreased, while a new absorption band at 287 nm appeared which was identical to that for the chloride substituted $[Pt_2(\mu\text{-pop})_4Cl_2]^{4-}$ (see later). In the presence of 2 equiv of Br^-, again two isosbestic points were observed when the spectra were collected during the course of oxidative electrolysis. The absorption bands observed after oxidative electrolysis at +300 mV are identical to those found with $[Pt_2(\mu\text{-pop})_4Br_2]^{4-}$ (see later). The oxidation process in the presence of Cl^- or Br^- (X^-) is therefore assigned to the overall reaction shown in eq 3, which represents a two-electron oxidation, rather than the one-electron process found in the absence of halide.

$$[Pt_2(\mu\text{-pop})_4]^{4-} + 2X^- \rightarrow [Pt_2(\mu\text{-pop})_4X_2]^{4-} + 2e^- \quad (3)$$

Controlled Potential Bulk Electrolysis. The current−time curve obtained during the course of attempted exhaustive bulk oxidative electrolysis of $[Pt_2(\mu\text{-pop})_4]^{4-}$ at +300 mV at a large surface area GC electrode decreased sharply in the early stages of the experiment and rapidly reached about 1% of the initial value. This behavior is very different from the exponential current decay that would be expected for a straightforward oxidation process. Moreover, the total charge consumed was only a small percentage of that required for a one-electron oxidation charge transfer process. The response is consistent with passivation of the electrode caused by adsorption, thus preventing further electron transfer.

Cyclic voltammograms obtained after the partial bulk oxidative electrolysis showed that the current magnitude had decreased in all the potential regions associated with oxidation of $[Pt_2(\mu\text{-pop})_4]^{4-}$ (Figure 5). There was a new reduction process at −2280 mV (not shown) that was irreversible over the scan rate range of 50 mV s^{-1} to 5 V s^{-1}. Qualitatively

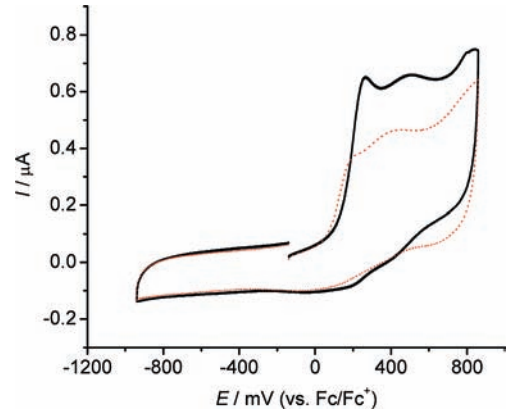

Figure 5. Cyclic voltammograms obtained before (black trace solid line) and after (red trace dotted line) attempted controlled potential bulk oxidative electrolysis of 0.5 mM $[Pt_2(\mu\text{-pop})_4]^{4-}$ at +300 mV.

similar observations were made at various concentrations of $[Pt_2(\mu\text{-pop})_4]^{4-}$ (2.0, 1.0, 0.5, and 0.1 mM). These data again confirm the complexity of oxidation of $[Pt_2(\mu\text{-pop})_4]^{4-}$ in weakly coordinating media.

Chemical Oxidation of $[Pt_2(\mu\text{-pop})_4]^{4-}$. Addition of $[NO][BF_4]$ to a 0.5 mM solution of $[PPN]_4[Pt_2(\mu\text{-pop})_4]$ in CH_2Cl_2 in the absence of air caused a rapid color change from pale greenish-yellow to light orange. Monitoring the reaction by spectrophotometry showed that the absorption band at 372 nm decreased in intensity and shifted to 363 nm. The cyclic voltammogram of the resulting solution showed removal of the first $[Pt_2(\mu\text{-pop})_4]^{4-}$ process, introduction of a new irreversible reduction process at about −2300 mV, while an oxidation peak was evident at +840 mV. These observations are consistent with those obtained after partial controlled potential bulk electrolysis and in spectroelectrochemical experiments. The oxidation of $[PPN]_4[Pt_2(\mu\text{-pop})_4]$ with $AgBF_4$ under similar conditions was very slow owing to the poor solubility of the latter in CH_2Cl_2, but the results obtained from cyclic voltammetry and UV−visible spectrophotometry were similar to those obtained by use of $[NO][BF_4]$.

On a preparative scale at higher concentrations (see Experimental Section), reaction of $[NO][BF_4]$ with either the PPN^+ or Bu_4N^+ salts of $[Pt_2(\mu\text{-pop})_4]^{4-}$ in a 1:1 mol ratio in CH_2Cl_2 caused immediate darkening of the solution and precipitation of a dark solid (**6**). Addition of ether to the supernatant liquid, in each case, precipitated orange solids, (**7a**) and (**7b**), respectively, whose ^{31}P NMR spectra in dichloromethane at room temperature showed no resonances due to complexed pyrophosphite. However, the ^{31}P NMR spectrum of **7a** contained the expected singlet at δ 21.6 due to the PPN^+ cation. Addition of an excess of $[Bu_4N]Cl$ to solutions of **7a** or **7b** caused an immediate color change to yellow, and the characteristic pattern of the diplatinum(III) anion **2a** was now evident in the ^{31}P NMR spectrum. Similarly, addition of $[Bu_4N]Br$ or $[Bu_4N]I$ to a solution of

(30) Le Suer, R. J.; Buttolph, C.; Geiger, W. E. *Anal. Chem.* **2004**, *76*, 6395.
(31) Bard, A. J.; Faulkner, L. R. *Electrochemical Methods: Fundamentals and Applications*; 2nd ed.; Wiley: New York, 2001.

7a gave yellow or orange solutions containing **2** (X = Br, I), together with unidentified peaks. Clearly, **7a** and **7b** contain platinum-μ-pyrophosphite species.

The IR spectra of **7a** and $[PPN]_4[Pt_2(\mu\text{-pop})_4]$ in KBr disks or Nujol mulls were generally similar, being dominated by bands due to PPN^+ and pyrophosphite. However, the spectrum of **7a** contained a band of medium intensity at about 1720 cm^{-1}, which was absent from the spectrum of $[PPN]_4[Pt_2(\mu\text{-pop})_4]$, and is reasonably assigned to the N−O stretching frequency of coordinated nitrosyl.[32−35] The IR spectrum of **7b** in Nujol also contained the same ν(NO) band at about 1720 cm^{-1}, but attempts to make a KBr disk caused a color change to blue, and the resulting IR spectrum showed no strong absorption in the 1700 cm^{-1} region. The PPN^+ derivative **7a** is stable under the same conditions.

Single-crystal X-ray diffraction analysis at −150 °C of a crystal grown from a solution of **7a** in CH_2Cl_2/ether (see below) has showed it to have the composition $[PPN]_3[Pt_2(\mu\text{-pop})_4(NO)]\cdot CH_2Cl_2\cdot 2Et_2O$; presumably **7b** contains the corresponding Bu_4N^+ salt. The anion is the product of a one-electron oxidation of $[Pt_2(\mu\text{-pop})_4]^{4-}$ by $[NO]^+$ (eq 4).

$$[cat]_4[Pt_2(\mu\text{-pop})_4] + [NO][BF_4] \rightarrow [cat]_3[Pt_2(\mu\text{-pop})_4(NO)] + [cat][BF_4] \quad (4)$$
$$cat^+ = Bu_4N^+, PPN^+$$

We were unable to obtain sufficient **7a** or **7b** for elemental analysis, and visual inspection suggested that these products, as obtained by slow crystallization with ether, contained a colorless solid, presumably the other reaction product, $[cat][BF_4]$. The presence of $[BF_4]^-$ should have been evident from its characteristic absorption at about 1000 cm^{-1} in the IR spectrum, but this region was dominated by bands arising from pop or PPN^+. In the following discussion, we shall label the pure PPN^+ salt of the nitrosyl anion as **8**.

Addition of $AgBF_4$ to a solution of $[PPN]_4[Pt_2(\mu\text{-pop})_4]$ precipitated an almost black solid, which appeared to be a mixture of **6** and metallic silver. The IR spectrum of **6**, obtained either from $[NO][BF_4]$ or $AgBF_4$, was very similar to that of **7a** except that the ν(NO) band was absent. However, the nature of **6**, which must be derived from the primary oxidation product $[Pt_2(\mu\text{-pop})_4]^{3-}$, remains unknown. The elemental analyses (see Experimental Section) were unexpectedly low in C and H, suggesting that PPN^+ may have been lost, but we could find no reasonable formulation. One possibility is that **6** is an oligomer of platinum(III) containing condensed pyrophosphite ligands, similar to the platinum(II) complexes formed from $K_4[Pt_2(\mu\text{-pop})_4]$ and phosphorous acid at 170 °C;[36] the XPS binding Pt energy (see later) is consistent with this possibility. Linear chains of alternating Pt(II)−Pt(III) or analogous square arrangements are also plausible.

Table 1. Selected Bond Distances (Å) and Angles (deg) for $[PPN]_3[Pt_2(\mu\text{-pop})_4(NO)]$ **8**

Pt(1)−Pt(2)	2.8375(6)	P(1)−Pt(1)−P(3)	88.23(11)
Pt(1)−P(1)	2.333(3)	P(1)−Pt(1)−P(5)	176.79(12)
Pt(1)−P(3)	2.334(3)	P(1)−Pt(1)−P(7)	91.96(12)
Pt(1)−P(5)	2.329(3)	P(3)−Pt(1)−P(5)	92.24(11)
Pt(1)−P(7)	2.328(3)	P(3)−Pt(1)−P(7)	176.56(11)
Pt(2)−P(2)	2.362(3)	P(5)−Pt(1)−P(7)	87.38(12)
Pt(2)−P(4)	2.357(3)	P(2)−Pt(2)−P(4)	87.29(12)
Pt(2)−P(6)	2.365(3)	P(2)−Pt(2)−P(6)	179.22(12)
Pt(2)−P(8)	2.353(4)	P(2)−Pt(2)−P(8)	92.95(13)
Pt(2)−N(1)	2.112(11)	P(4)−Pt(2)−P(6)	105.52(8)
		P(4)−Pt(2)−P(8)	92.76(13)
P═O, P−OH	1.510(9)−1.550(9)	P(6)−Pt(2)−P(8)	86.98(15)
P−O−P	1.592(10)−1.644(10)	N(1)−Pt(2)−P(2)	93.3(3)
		N(1)−Pt(2)−P(4)	88.7(3)
		N(1)−Pt(2)−P(6)	86.0(3)
		N(1)−Pt(2)−P(8)	90.0(3)
		N(1)−Pt(2)−Pt(1)	175.9(3)

Structural Characterization and Formulation of the Nitrosyl Complex 8. The fairly poor quality of the crystal limited the precision of the final structure but was sufficient to establish the atom connectivity and the main features. The molecular structure of the anion is shown in Figure 6; selected bond distances and angles are listed in Table 1.

The anion contains the usual $Pt_2(\mu\text{-pop})_4$ framework. One platinum atom, Pt(2), is attached to an N-bonded, bent nitrosyl group in the axial position, the Pt−N−O angle being 118.1(12)° and the N−O distance 1.111(15) Å; the N(1)−Pt(2)−Pt(1) angle is 176.0(3)°. The corresponding axial position for Pt(1) is blocked by a phenyl group of one of the PPN^+ cations (Pt−C distance ca. 3.2 Å).

The anion in **8** thus differs from all the diplatinum(III)-pop complexes reported so far in possessing only one axial ligand. Moreover, the composition of **8** differs from those of **1**−**4** in the presence of three counter-cations per anion. Most of the known examples have either four, as in **1**−**4**, or two, as in the diplatinum(III) anions $[Pt_2(\mu\text{-pop})_4L_2]^{2-}$ (L =

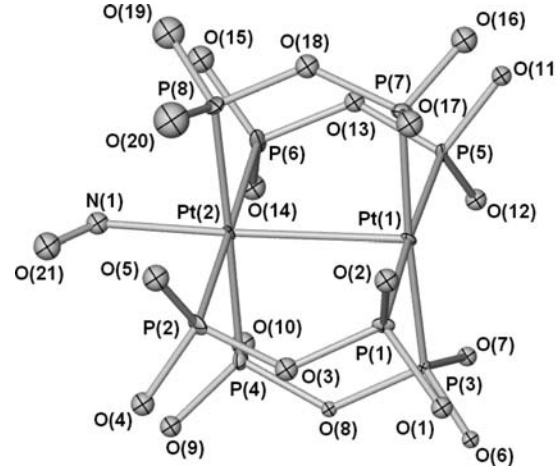

Figure 6. Molecular structure of the $[Pt_2(\mu\text{-pop})_4(NO)]^{3-}$ anion of $[PPN]_3[Pt_2(\mu\text{-pop})_4(NO)]\cdot 2Et_2O\cdot CH_2Cl_2$. Hydrogen atoms have been omitted for clarity and only one component of the disordered NO moiety is shown.

(32) Johnson, B. F. G.; Haymore, B. L.; Dilworth, J. R. In *Comprehensive Coordination Chemistry*; Wilkinson, G., Gillard, R. D., McCleverty, J. A., Eds.; Pergamon: Oxford, 1987; Vol. 2, p 99.
(33) Mingos, D. M. P.; Sherman, D. J. *Adv. Inorg. Chem.* **1989**, *34*, 293.
(34) Richter-Addo, G. B.; Legzdins, P., *Metal Nitrosyls*; Oxford University Press: New York, 1992; pp 61−68.
(35) Hayton, T. W.; Legzdins, P.; Sharp, W. B. *Chem. Rev.* **2002**, *102*, 935.
(36) Dickson, M. K.; Fordyce, W. A.; Appel, D. M.; Alexander, K. A.; Stein, P.; Roundhill, D. M. *Inorg. Chem.* **1982**, *21*, 3858.
(37) Che, C.-M.; Miskowski, V. M.; Mak, T. C. W.; Gray, H. B. *J. Am. Chem. Soc.* **1986**, *108*, 7840.
(38) Che, C.-M.; Lee, W.-M.; Mak, T. C. W.; Gray, H. B. *J. Am. Chem. Soc.* **1986**, *108*, 4446.

MeCN, imidazole, Et_2S).[37−39] There are salts of [Pt_2(μ-pop)$_4$]$^{4-}$ that contain only two or three organic cations per anion in which charge balance is maintained by addition of one or two protons to the oxygen atoms of the P═O groups, for example, [Et_4N]$_3$[Pt_2(μ-pop)$_3$(μ-popH)][40] and [cat]$_2$[Pt_2(μ-pop)$_2$(μ-popH)$_2$] [cat$^+$ = Bu_4N^+, $(PhCH_2)Et_3N^+$ or $(PhCH_2)$-Bu_3N^+].[41] In these compounds, the P−O distances corresponding to the P═O and P−OH groups tend to fall into two groups, about 1.50−1.53 Å and 1.55−1.58 Å, respectively. We modeled the structure of **8** with unprotonated $[P_2O_5H_2]^{2-}$ ligands, although the remaining hydrogen atom positions were not located. The narrow range observed for the P−O distances [1.517(10)−1.550(9) Å, the variation being less than the 3σ limit] is consistent with the absence of additional protonation of the oxygen atoms. The data suggest that the P−OH and P═O groups may be disordered, but attempts to model this possibility were unsuccessful.

For the purpose of electron accounting in redox reactions, it is often helpful to assign oxidation numbers to the metal atoms, but this can be a contentious matter in nitrosyl complexes. The problem is often avoided by use of the Enemark−Feltham notation[42] in which the unpaired electron of each NO ligand is counted in with the metal d-electrons; thus, the nitrosyl-bearing platinum atom in **8** can be labeled as {Pt(NO)}. Recognizing that oxidation numbers are purely formal, we think that the marked nonlinearity of the Pt−NO linkage in **8** is most consistent with the formulation $[NO]^-$ for the ligand. On this basis, the *average* oxidation number of the platinum atoms in **8** is +3 and the formation of **8** can be viewed as an overall one-electron oxidation of the diplatinum(II) complex **1** accompanied by ligand transfer (eq 4). The mechanism of the process is unknown, but initial oxidation to the transient species [Pt_2(μ-pop)$_4$]$^{3-}$ and subsequent addition of the byproduct NO appears to be plausible. The alternative $[NO]^+$ formulation leads to the apparently reasonable oxidation number +2 for each platinum atom but implies, less reasonably, that the process by which **8** is formed is not an oxidation.

The Pt−Pt distance in **8** [2.8375(6) Å] is less than that in its diplatinum(II) precursor **1** [2.925(1) Å],[2] as expected for an oxidation process, but falls beyond the range of distances observed in the axially disubstituted diplatinum(III) complexes [Pt_2(μ-pop)$_4$X$_2$]$^{4-}$ (X = Cl, Br, I, SCN, NO_2) [2.695(1)−2.794(1) Å][7,8,11,12,18,38] and [Pt_2(μ-pop)$_4$L$_2$]$^{2-}$ (L = MeCN, 2.676(1) Å;[37] L = imidazole, 2.745(1) Å;[38] L = Et_2S, 2.766(1) Å[39]]. It is very close to the Pt−Pt distances in the mixed-valent Pt(II)−Pt(III) complexes **4**, for example, K_4[Pt_2(μ-pop)$_4$(μ-Cl)]·3H_2O [2.813(1) Å],[12] K_4[Pt_2(μ-pop)$_4$(μ-X)]·2H_2O [2.835(1) Å for X = Cl; 2.834(1) Å for X = Br],[18] and [NH_4]$_4$[Pt_2(μ-pop)$_4$(μ-Cl)] [2.830(1) Å].[17] This similarity could provide support for regarding **8** similarly as a Pt(II)−Pt(III) complex, a view that would also be consistent with the XPS data (see below). However, to maintain consistency with the oxidation state argument presented above, we prefer to regard **8** as a diplatinum(III) complex, like **2a**-**c**, in which the axial ligand, NO^-, which is known to have a high *trans*-influence,[43] weakens the Pt−Pt bond and destabilizes axial coordination at the second platinum atom, Pt(1). This representation is shown in Figure 7a.

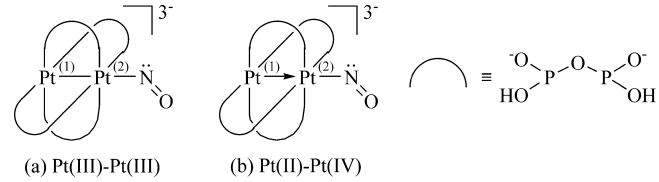

(a) Pt(III)-Pt(III) (b) Pt(II)-Pt(IV)

Figure 7. Alternative representations of [Pt_2(μ-pop)$_4$(NO)]$^{3-}$.

An alternative view that maintains the average oxidation number of +3 is to regard Pt(1) as being divalent and Pt(2) as tetravalent, five-coordinate platinum(IV), with a donor−acceptor bond from Pt(II) to Pt(IV), as shown in Figure 7b.

The Pt−NO distance in **8**, 2.112(11) Å, is comparable with the corresponding distance in three, precisely determined, five-coordinate {Pt(NO)}^{8} structures, namely, [Bu_4N][$PtCl_2$-$(C_6Cl_5)_2$(NO)] [2.054(9) Å],[44] [$Pt(C_6F_5)_3(PMe_2Ph)$(NO)] [2.068(7) Å][45] and [PPN][$Pt(C_6F_5)_4$(NO)] [2.035(4) Å].[45] The platinum atoms in these compounds are in a square pyramidal coordination environment, as is Pt(2) in **8**, and the Pt−N−O angles are 119.5(8)°, 120.1(6)°, and 130.2(6)°, respectively, similar to that in **8**. Theoretical calculations predict a bent M−N−O unit for square pyramidal metal nitrosyl complexes with a {M(NO)}^{8} configuration[46] and only the [$Pt(C_6Cl_5)_4$-(NO)]$^-$ anion appears to be exceptional in this class of compound in having a linear Pt−NO group,[47] possibly because of electrostatic effects in the second sphere environment.[45] There are also four, less precisely determined structures of closely related complexes containing a six-coordinate {Pt(NO)}^{8} unit, namely, [NEt_4]$_2$[$PtCl_2$(μ-NO)(μ-Cl)$PtCl_3$(NO)],[48] [quin]$_2$[Pt_2Cl_6(μ-Cl)$_2$(NO)$_2$][49] [quin = quinolinium, $C_9H_7NH^+$], K_2[$Pt(NO_2)_2Cl_3$(NO)],[50] and K[$Pt(NO_2)_4$-(NO)(H_2O)]·H_2O.[50] In all these cases, the terminal NO ligands are bent, the Pt−N−O angles being 122(5)°, 112°, 119(2)°, and 125° (weighted average), respectively. Moreover, the Pt−Cl distances *trans* to bent NO are very long [2.62(1) Å, 2.74(1) Å, and 2.562(5) Å, respectively, in the first three compounds], indicative of the high *trans*-influence of bent NO.

(39) Che, C.-M.; Cheng, M.-C.; Wang, Y.; Gray, H. B. *Inorg. Chim. Acta* **1992**, *191*, 7.
(40) Kim, C. D.; Pillet, S.; Wu, G.; Fullagar, W. K.; Coppens, P. *Acta Crystallogr., Sect. A* **2002**, *58*, 133.
(41) Yasuda, N.; Uekusa, H.; Ohashi, Y. *Bull. Chem. Soc. Jpn.* **2004**, *77*, 933.
(42) Enemark, J. H.; Feltham, R. D. *Coord. Chem. Rev.* **1974**, *13*, 339.
(43) Reference 34, pp 50−52, 91−93, 183.
(44) Forniés, J.; Menjón, B.; Sanz-Carillo, R. M.; Tomás, M. *Chem. Ber.* **1994**, *127*, 651.
(45) Ara, I.; Forniés, J.; García-Monforte, M. A.; Menjón, B.; Sanz-Carillo, R. M.; Tomás, M.; Tsipis, A. C.; Tsipis, C. A. *Chem.—Eur. J.* **2003**, *9*, 4094.
(46) Hoffmann, R.; Chen, M. M.; Elian, M.; Rossi, A. R.; Mingos, D. M. P. *Inorg. Chem.* **1974**, *13*, 2666.
(47) Usón, R.; Forniés, J.; Tomás, M.; Menjón, B.; Bau, R.; Sünkel, K.; Kuwabara, E. *Organometallics* **1986**, *5*, 1576.
(48) Epstein, J. M.; White, A. H.; Wild, S. B.; Willis, A. C. *J. Chem. Soc., Dalton Trans.* **1974**, 436.
(49) Khodashova, T. S.; Sergienko, V. S.; Stetsenko, A. N.; Porai-Koshits, M. A.; Butman, L. A. *Zh. Strukt. Khim.* **1974**, *15*, 471. *Russ. J. Struct. Chem.* **1974**, *15*, 402.
(50) Peterson, E. S.; Larsen, R. D.; Abbott, E. H. *Inorg. Chem.* **1988**, *27*, 3514.

NMR Spectroscopy. Since no ^{31}P NMR resonances due to the pop ligands could be observed at room temperature, we thought at first that the anion of **8**, present as the main component of **7a**, must be paramagnetic. However, no EPR signals were observed, even at liquid helium temperature, and magnetic susceptibility measurements on a solid sample were not decisive owing to the large diamagnetic contributions of the PPN^+ cations. When a solution of **7a** in CD_2Cl_2 was cooled to 183 K, two equally intense quintets, accompanied by less well resolved ^{195}Pt satellites, appeared at δ 43.7 [J(PP) 12.9 Hz, J(PtP) ca. 2570 Hz] and δ 73.0 [J(PP) 12.8 Hz, J(PtP) ca. 2708 Hz], which can be assigned to the inequivalent phosphorus atoms of coordinated pop; there was also a broad resonance at about δ 67−68 possibly arising from **1**. The resonances collapsed into the baseline as the solution was warmed and reappeared on cooling. In solution, therefore, the NO group of **7a** appears to migrate rapidly on the NMR time-scale at room temperature, causing the platinum atoms to become equivalent. We do not know whether this occurs by rapid, reversible dissociation of NO or whether the process is intramolecular.

We tentatively assign the resonance at δ 73.0 to the phosphorus atoms on the four-coordinate atom Pt(1), because of the similarity of the chemical shift and Pt−P coupling constant to those of $[PPN]_4[Pt_2(\mu\text{-pop})_4]$ [δ 67.7, J(PtP) 3019 Hz], in which the phosphorus atoms are in a similar environment. The smaller Pt−P coupling constant for the phosphorus atoms on Pt(2), which bears the nitrosyl group, is consistent with the higher coordination number of this atom. Both the chemical shift and J(PtP) value for these phosphorus atoms differ considerably from those in the diplatinum(III) complexes of type **2** [δ 20−30, J(PtP) ca. 2050 Hz] and from those in the mixed-valent complexes of type **5** in the solid state [e.g., for X = I, δ 19 ± 2.6 and J(PtP) 2300 ± 50 Hz]; hence, the ^{31}P NMR data of **7a** provide no firm guide to the formal oxidation numbers of the platinum atoms.

X-Ray Photoelectron Spectroscopy (XPS). The platinum $4f_{7/2}$ binding energy in platinum complexes increases by about 1.1 eV for each unit increase in the formal oxidation state of the metal atoms, although ligand effects in complexes of the same oxidation state can be almost as large.[51−56] The XP spectrum of the diplatinum(II) complex $[Bu_4N]_4[Pt_2(\mu\text{-pop})_4]$ (**1**) shows a typical $4f_{7/2}/4f_{5/2}$ doublet, the binding energy of the $4f_{7/2}$ peak being 72.0 eV; the spectra of the diplatinum(III) complexes $[Bu_4N]_4[Pt_2(\mu\text{-pop})_4X_2]$ (**2a-c**) are similar, the binding energies of the $4f_{7/2}$ peaks (in eV) being 73.5 (X = Cl), 73.2 (X = Br), and 73.1 (X = I). Although the trend in binding energies is similar, the values are consistently lower by about 1 eV than those reported[10] for the same anions with different cations, namely, $K_4[Pt_2(\mu\text{-pop})_4]\cdot 2H_2O$ (**1**) (73.7 eV), $K_4[Pt_2(\mu\text{-pop})_4Cl_2]\cdot 2H_2O$ (**2a**) (75.1 eV), $K_4[Pt_2(\mu\text{-pop})_4Br_2]$ (**2b**) (74.5 eV), $[Ph_4As]_4[Pt_2(\mu\text{-pop})_4I_2]$ (**2c**) (73.7 eV). The reason for these discrepancies is not clear; we note, however, that our value for $[Bu_4N]_4[Pt_2(\mu\text{-pop})_4]$ (**1**) agrees well with the values reported[19] for the Pt(II) ions in the localized mixed-valent species $[cat]_4[Pt_2(\mu\text{-pop})_4I]$ [$cat^+ = NH_4^+$ (72.17 eV at 77 K), Cs^+ (72.26 eV at room temperature)] and that our value for **2c** is in reasonable agreement with the values reported for the Pt(III) ions in the same complexes [$cat^+ = NH_4^+$ (73.22 eV at 77 K), Cs^+ (73.48 eV at room temperature)]. We have remeasured the XP spectra of the potassium salts of complexes **1** and **2a**, and find the expected Pt $4f_{7/2}$ doublets at 72.3 and 73.5 eV, respectively, almost identical to the results obtained for the Bu_4N^+ analogues, indicating that the cation has little effect on the platinum binding energies.

The XP spectrum of the complex $[Bu_4N]_3[Pt_2(\mu\text{-pop})_4(NO)]$ showed two, poorly resolved $4f_{7/2}$ peaks with binding energies of 73.7 and 72.3 eV, thus confirming the inequivalence of the two platinum atoms. The lower energy peak can be reasonably assigned to the planar-coordinated platinum atom Pt(1) because the binding energy is the same as that of the divalent platinum atom in **1**; the higher energy peak must then be assigned to the nitrosyl-bearing platinum atom Pt(2). Although its binding energy is in the range observed for the diplatinum(III) complexes **2a-c**, the value does not exclude the assignment of a formal oxidation state of +4 if one allows the possibility of a marked effect on the binding energy of the strongly σ-donating NO^- ligand, with its high *trans*-influence. Binding energies for octahedral platinum(IV) complexes range from 77.8 eV for K_2PtF_6 to 73.6 eV for K_2PtI_6;[53−55] in platinum(II) complexes, successive replacement of the chloride ligands of $[PtCl_2(PEt_3)_2]$ by strongly σ-donating methyl groups causes the Pt $4f_{7/2}$ binding energies to fall from 73.3 to 72.8 eV for $[PtClMe(PEt_3)_2]$ to 72.4 eV for $[PtMe_2(PEt_3)_2]$.[52] Unfortunately, so far as we know, there are no XP measurements on well-defined platinum-nitrosyl complexes available for comparison.[57] The dark, insoluble material **6** also produced during the NO^+ oxidation of $[Bu_4N]_4[Pt_2(\mu\text{-pop})_4]$ showed a single Pt $4f_{7/2}$ peak at 73.4 eV in its XP spectrum, similar to those of the dihalo complexes $[Bu_4N]_4[Pt_2(\mu\text{-pop})_4X_2]$ above, strongly suggestive of Pt(III); the absence of a second peak excludes the possibility of a mixed-valent species similar to **8**.

The XP spectrum of the product of oxidation of **1** with $AgBF_4$ showed a typical doublet with the Pt $4f_{7/2}$ peak at 73.6 eV, consistent with the presence of platinum(III) (for this series of compounds), but this overlapped a second doublet with a $4f_{7/2}$ peak at 71.4 eV, possibly because of metallic platinum displaced by the $AgBF_4$ (literature value 71.3 eV).[51−54]

(51) Cook, C. D.; Wan, K. Y.; Gelius, U.; Hamrin, K.; Johansson, G.; Olsson, E.; Siegbahn, H.; Nordling, C.; Siegbahn, K. *J. Am. Chem. Soc.* **1971**, *93*, 1904.
(52) Riggs, W. M. *Anal. Chem.* **1972**, *44*, 830.
(53) Moddeman, W. E.; Blackburn, J. R.; Kumar, G.; Morgan, K. A.; Albridge, R. G.; Jones, M. M. *Inorg. Chem.* **1972**, *11*, 1715.
(54) Nefedov, V. I.; Salyn, Y. V. *Inorg. Chim. Acta* **1978**, *28*, L135.
(55) Barton, J. K.; Best, S. A.; Lippard, S. J.; Walton, R. A. *J. Am. Chem. Soc.* **1978**, *100*, 3785.
(56) Muisjers, J. C.; Niemandsverdriet, J. W.; Wehman-Ooyevaar, I. C. M.; Grove, D. M.; van Koten, G. *Inorg. Chem.* **1992**, *31*, 2655.

(57) Evaporation to dryness of the solution from which a single crystal of $K[Pt(NO_2)_4(NO)(H_2O)]\cdot H_2O$ had been grown gave a blue powder, the XP spectrum of which showed two sets of Pt $4f_{7/2}/4f_{5/2}$ doublets of approximately equal intensity.[50] The $4f_{7/2}$ binding energies of 72.9 and 75.2 eV correspond to Pt(II) and Pt(IV), respectively, but the nature of the two species has not been established.

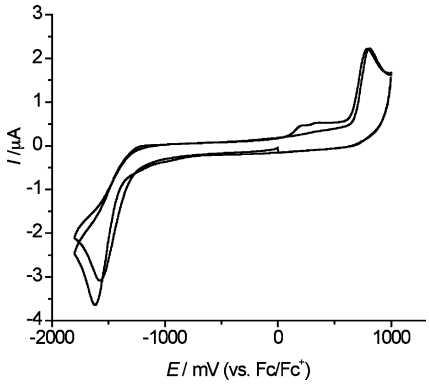

Figure 8. Cyclic voltammogram for the reduction of 1.0 mM [Pt$_2$(μ-pop)$_4$Cl$_2$]$^{4-}$ at 20 °C using a glassy carbon electrode and a scan rate of 100 mV s^{-1}.

Electrochemical Reduction of the Axially Substituted Diplatinum(III) Complexes [Pt$_2$(μ-pop)$_4$X$_2$]$^{4-}$. Voltammetric Studies. The Bu$_4$N$^+$ salts of [Pt$_2$(μ-pop)$_4$X$_2$]$^{4-}$ all exhibited an irreversible reduction process under conditions of cyclic voltammetry at a glassy carbon electrode, with peak potentials at about −1600, −1400, and −1200 mV for X = Cl, Br, I, respectively. When the scan direction was reversed, a new oxidation process was observed for all the halides at about +200 mV. Thus, the oxidative process coupled to the reduction of [Pt$_2$(μ-pop)$_4$X$_2$]$^{4-}$ is independent of the halide in the poorly coordinating solvent dichloromethane and occurs at the same potential as found for the initial oxidation of [Pt$_2$(μ-pop)$_4$]$^{4-}$. This process is attributed to oxidation of [Pt$_2$(μ-pop)$_4$]$^{4-}$ formed as a product of reduction of [Pt$_2$(μ-pop)$_4$X$_2$]$^{4-}$, and not from [Pt$_2$(μ-pop)$_4$X$_2$]$^{4-}$ present initially in solution, since no oxidation current is detected in this region when the potential is initially scanned in the positive direction (Figure 8). The anions [Pt$_2$(μ-pop)$_4$X$_2$]$^{4-}$ (X = Cl, Br, I) also exhibited an irreversible oxidation process at about 800−850 mV, the potential being similar to that of the second oxidation process of [Pt$_2$(μ-pop)$_4$]$^{4-}$. This feature is characteristic of all the compounds in this series.

In Situ Spectroelectrochemical Studies. In situ spectroelectrochemical studies of the reduction of [Pt$_2$(μ-pop)$_4$Cl$_2$]$^{4-}$ at a platinum gauze electrode in dichloromethane at room temperature showed that the intensity of the absorption bands at 287 and 349 nm decreased when the potential was held at −1800 mV, while a new band appeared at 372 nm, which is assigned to [Pt$_2$(μ-pop)$_4$]$^{4-}$ formed by reduction. The bromo and iodo analogues behaved similarly. On reductive electrolysis of [Pt$_2$(μ-pop)$_4$Br$_2$]$^{4-}$ at −1600 mV, the absorbances of the bands at 302 and 362 nm (shoulder) decreased, while a new band due to [Pt$_2$(μ-pop)$_4$]$^{4-}$ appeared at 372 nm. Electroreduction of the iodo analogue at −1400 mV caused its bands at 276, 339, and 437 nm to disappear and their replacement by the band at 372 nm. In all three cases, reoxidation of the reduced solutions at +300 mV regenerated quantitatively the original [Pt$_2$(μ-pop)$_4$X$_2$]$^{4-}$ species. Thus, the redox cycles are chemically reversible in dichloromethane (eq 5), the behavior being similar to that in coordinating solvents (see Introduction). The solvent plays a decisive role only in the oxidation of [Pt$_2$(μ-pop)$_4$]$^{4-}$ in the absence of halide.

$$[Pt_2(\mu\text{-pop})_4X_2]^{4-} + 2e^- \rightleftharpoons [Pt_2(\mu\text{-pop})_4]^{4-} + 2X^- \quad (5)$$

Controlled Potential Bulk Reductive Electrolysis. To confirm that the reduction is a two-electron process, a controlled potential bulk electrolysis experiment was carried out at −1600 mV for the reduction of [Pt$_2$(μ-pop)$_4$Br$_2$]$^{4-}$ in dichloromethane at room temperature. The resultant current−time curve obtained exhibited the expected exponential current decay. Coulometric analysis of these data gave an n value of 1.92 (±0.02) electrons per molecule. The solution changed from dark yellow to pale yellow upon reduction. Cyclic voltammetric measurements made after bulk electrolysis revealed that the oxidation process detected on reverse scans prior to bulk electrolysis (Figure 9a) was now present as the primary oxidation process. The electronic spectrum of the reduction product (Figure 9b) has absorption bands at 246, 312, and 372 nm as expected for [Pt$_2$(μ-pop)$_4$]$^{4-}$ in dichloromethane. The bulk electrolysis data are consistent with the spectroelectrochemical results and eq 4. Controlled potential bulk reductive electrolysis of [Pt$_2$(μ-pop)$_4$Cl$_2$]$^{4-}$ and [Pt$_2$(μ-pop)$_4$I$_2$]$^{4-}$ in dichloromethane at room temperature are also consistent with the spectroelectrochemical results and eq 5.

Voltammetric and Spectrophotometric Studies on Mixtures of [Pt$_2$(μ-pop)$_4$]$^{4-}$ and [Pt$_2$(μ-pop)$_4$Br$_2$]$^{4-}$. In an equimolar mixture of [Pt$_2$(μ-pop)$_4$]$^{4-}$ and [Pt$_2$(μ-pop)$_4$Br$_2$]$^{4-}$, both cyclic voltammograms and UV−visible spectra contain the summed features of [Pt$_2$(μ-pop)$_4$]$^{4-}$ and [Pt$_2$(μ-pop)$_4$Br$_2$]$^{4-}$ (Supporting Information, Figure S2). This confirms that the mixed-valent species [Pt$_2$(μ-pop)$_4$Br]$^{4-}$ (see Introduction) is not present in a significant concentration in a mixture of [Pt$_2$(μ-pop)$_4$]$^{4-}$ and [Pt$_2$(μ-pop)$_4$Br$_2$]$^{4-}$ in dichloromethane.

Discussion

On the cyclic voltammetric time-scale, oxidation of [Pt$_2$(μ-pop)$_4$]$^{4-}$ (**1**) in dichloromethane resembles that in water or acetonitrile in being a one-electron process. However, in the more weakly coordinating dichloromethane, the transient one-electron oxidation product, [Pt$_2$(μ-pop)$_4$]$^{3-}$ (**5**), rearranges to an ill-defined, probably oligomeric product (**6**) that appears to contain Pt(III). By contrast, in water or acetonitrile, ligand addition is followed by disproportionation, which occurs on a longer time-scale in the coordinating environment. The reversible potentials for the [Pt$_2$(μ-pop)$_4$]$^{3-/4-}$ and [Pt$_2$(μ-C$_6$H$_3$-5-Me-2-AsPh$_2$)$_4$]$^{+1/0}$ couples (+203 mV and −165 mV, respectively) clearly show the greater resistance of the pop anion to oxidation, despite the presence of the negative charge, which is probably a consequence of the strong electron-withdrawing properties of the pyrophosphite ligands.

Although treatment of **1** with [NO][BF$_4$] gives mainly **6**, some of the transient **5** is captured by NO to give the unprecedented anion [Pt$_2$(μ-pop)$_4$(NO)]$^{3-}$ (**8**). Previous attempts to form nitrosyl complexes containing the Pt$_2$(μ-pop)$_4$ unit have failed.[58] For example, NO was reported not to react

(58) Hedden, D.; Roundhill, D. M.; Walkinshaw, M. D. *Inorg. Chem.* **1985**, *24*, 3146.

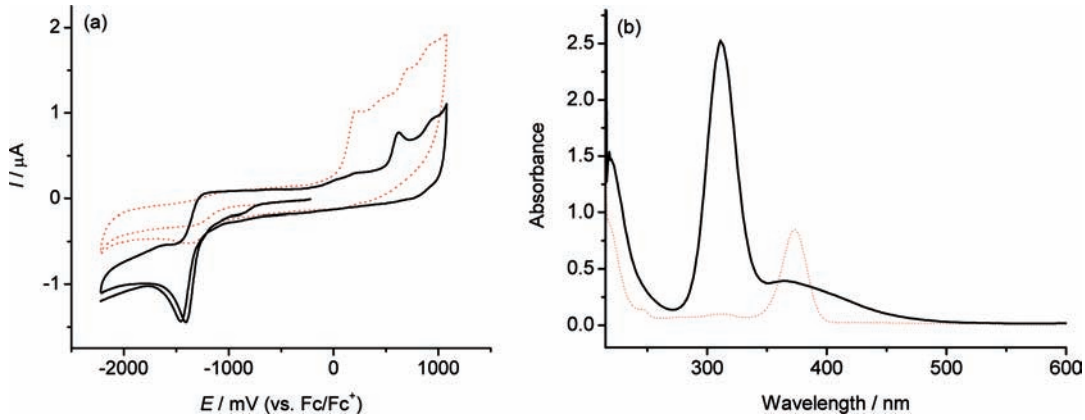

Figure 9. Comparison of cyclic voltammograms (a) and UV−visible spectra (b) of 0.5 mM $[Pt_2(\mu\text{-pop})_4Br_2]^{4-}$ in dichloromethane before (black trace solid line) and after (red trace dotted line) controlled-potential bulk electrolysis at −1600 mV at room temperature.

with **1** in aqueous solution, NOCl added to **1** in aqueous solution to give only $[Pt_2(\mu\text{-pop})_4Cl_2]^{4-}$ (**2a**), and CO reacted with the nitro-complex $[Pt_2(\mu\text{-pop})_4(NO_2)_2]^{4-}$ in aqueous solution to give **1**, NO and CO_2. It has been suggested, therefore, that the platinum atoms in **1** are too electron-poor to accommodate the strong π-acceptor NO,[58] but this conclusion is clearly incorrect. Our synthetic result shows a superficial resemblance to the oxidation of the diplatinum(I) complex $[Pt_2Cl_2(\mu\text{-dppm})_2]$ (dppm = $Ph_2PCH_2PPh_2$) by $[NO]^+Y^-$ (Y = BF_4, PF_6), but, in contrast to **8**, the product of this reaction, the A-frame complex $[Pt_2Cl_2(\mu\text{-dppm})_2(\mu\text{-NO})]Y$, contains a bridging, non-fluxional NO ligand.[59,60]

An important factor in the isolation of $[Pt_2(\mu\text{-pop})_4(NO)]^{3-}$ is probably the use of salts containing large, stabilizing organic cations, such as Bu_4N^+ and PPN^+, in non-aqueous, non-coordinating media. In support of this suggestion, we have observed that $[PPN]_4[Pt_2(\mu\text{-pop})_4]$ in CH_2Cl_2 reacts directly with NO to give an as yet uncharacterized nitrosyl species, different from **8**, which shows a ν(NO) band at about 1735 cm^{-1} in its IR spectrum.

In contrast to the solvent-dependent oxidation of $[Pt_2(\mu\text{-pop})_4]^{4-}$, reduction of $[Pt_2(\mu\text{-pop})_4X_2]^{4-}$ in poorly coordinating dichloromethane is analogous to the chemically reversible, electrochemically irreversible overall two-electron reduction reaction found in coordinating solvents.

Experimental Section

Reagents and Starting Materials. Dichloromethane (HPLC grade, Merck) was dried over basic alumina before use. The supporting electrolyte $[Bu_4N][PF_6]$ (98%, GFS Chemicals) was recrystallized twice from ethanol,[61] and $[Bu_4N][BArF_{24}]$ and $[Bu_4N][B(C_6F_5)_4]$ provided by Dr. Matthew Byrnes and Dr. Ayman Nafady, respectively. Ferrocene, nitrosonium tetrafluoroborate ($[NO][BF_4]$), $[Bu_4N]X$ (X = Cl, Br, I), and bis(triphenylphosphine)iminium chloride ([PPN]Cl) were obtained commercially and used as received. The salt $K_4[Pt_2(\mu\text{-pop})_4]\cdot 2H_2O$ was prepared as described[10] in about 35% yield.

Instrumentation and Procedures. ^{31}P NMR spectra were recorded at 121 MHz on a Bruker Aspect 2000 and low temperature ^{31}P NMR spectra at 162 MHz on a Varian Unity Plus spectrometer with use of H_3PO_4 (85% in D_2O) as external reference (set at 0 ppm). IR spectra (KBr disks and Nujol mulls) were measured on a Perkin-Elmer Spectrum 2000 FT spectrometer. XPS data were obtained on a VG Microlab 310F spectrometer with an unmonochromated, aluminum anode X-ray source operated at a power of 300 W and 15 kV excitation voltage and are referenced to the C 1s peak at 285.0 eV.

Electrochemical experiments were carried out in a standard three-electrode arrangement with a Bioanalytical Systems BAS Model 100B electrochemical workstation (Bioanalytical Systems, West Lafayette, IN, U.S.A.). A Pt wire auxiliary electrode and a Ag/AgCl (CH_2Cl_2, 0.1 M $[Bu_4N][PF_6]$) single junction quasi-reference electrode were used for voltammetric studies in dichloromethane, although the potentials are quoted relative to the Fc/Fc^+ potential scale. The same reference electrode was used with the other electrochemical techniques employed in dichloromethane, but an aqueous Ag/AgCl (3 M NaCl) solution was used for studies in water. Glassy carbon (GC), Au, or Pt working electrodes with a diameter of 0.10 cm and an area of 0.0079 cm^2 were used for cyclic voltammetric experiments; the GC working electrode used for rotating disk experiments had a diameter of 0.30 cm and an area of 0.071 cm^2 and was used with a BAS RDE-2 accessory. An 11 μm diameter glassy carbon microelectrode was used as the working electrode for fast scan rate microelectrode voltammetric studies. The areas or radii of the voltammetric working electrodes were determined by reduction of 1.0 mM $[Ru(NH_3)_6]^{3+}$ (diffusion coefficient of 6.2×10^{-6} cm^2 s^{-1}) in water (0.5 M KCl) and the application of the relevant equations, that is, the Randles−Sevcik equation for the transient voltammetry with macrodisk electrodes, the steady-state diffusion limiting current equation for the microdisk electrode voltammetry, and the Levich equation for the RDE voltammetry.[31] For spectroelectrochemical studies, a platinum gauze electrode working electrode and a platinum wire auxiliary electrode separated from the platinum gauze electrode by a fine porosity frit were used. In the case of bulk electrolysis experiments, a glassy carbon tube working electrode and a platinum gauze auxiliary electrode, separated from the test solution by a fine porosity frit, were used. Prior to each voltammetric experiment, the working electrode was polished with 0.3 μm alumina on a clean polishing cloth (Buehler, U.S.A.), rinsed with water, then acetone and finally dried with tissue paper. The solutions used for voltammetric,

(59) Ghedini, M.; Neve, F.; Mealli, C.; Tiripicchio, A.; Ugozzoli, F. *Inorg. Chim. Acta* **1990**, *178*, 5.
(60) Neve, F.; Ghedini, M.; Tiripicchio, A.; Ugozzoli, F. *Organometallics* **1992**, *11*, 796.
(61) Sawyer, D. T.; Sobkowiak, A.; Roberts, J. L. J. *Electrochemistry for Chemists*, 2nd ed.; Wiley: New York, 1995.

Table 2. Analytical[a] and ^{31}P NMR Data[b] for [Bu$_4$N]$_4$[Pt$_2$(μ-pop)$_4$X$_2$] [X = Cl (**2a**), Br (**2b**), I (**2c**)]

	%C	%H	%N	%X	δ [*J*(PtP)]
2a	37.40 (38.46)	6.91 (7.26)	2.46 (2.80)	4.10 (3.55)	30.0 (2049)[c]
2b	35.01 (36.82)	6.46 (6.95)	2.33 (2.68)		26.3 (2052)[d]
2c	35.10 (35.24)	6.95 (6.65)	2.42 (2.57)	12.06 (11.63)	20.3 (2069)[e]

[a] Calculated values in parenthesis. [b] Coupling constants in hertz. [c] Literature[7,10] K$_4$[Pt$_2$(μ-pop)$_4$Cl$_2$] in H$_2$O: δ 28.0 (2085 Hz). [d] Literature[7,10] K$_4$[Pt$_2$(μ-pop)$_4$Br$_2$] in H$_2$O: δ 24.0 (2100 Hz). [e] Literature[7,10] K$_4$[Pt$_2$(μ-pop)$_4$I$_2$] in H$_2$O: δ 18.0 (2148 Hz); [Ph$_4$As]$_4$[Pt$_2$(μ-pop)$_4$I$_2$] (solvent not specified): δ 18.2 (2200 Hz).

spectroelectrochemical, and bulk electrolysis measurements were purged with solvent-saturated nitrogen gas before each experiment and were blanketed with nitrogen gas during the experiment.

UV−visible spectra over the wavelength range from 200 to 800 nm were recorded continuously during the course of the electrolysis in spectroelectrochemical experiments at a scan rate of 600 nm min^{-1} until the electrolysis was completed. All electrochemical studies were carried out at either room temperature (20 ± 2 °C) or low temperature (−75 ± 2 °C), the latter being achieved by immersing the cell in an acetone/dry ice mixture.

Preparations. [Bu$_4$N]$_4$[Pt$_2$(μ-pop)$_4$]. The literature procedure[10] was modified. A solution of K$_4$[Pt$_2$(μ-pop)$_4$] (0.32 g, 0.28 mmol) in water (4 mL) was treated with a large excess of [Bu$_4$N]Cl to give a thick syrup, which was extracted with CH$_2$Cl$_2$ (3 × 50 mL). The yellow organic layer was separated and evaporated to small volume under reduced pressure. Addition of ethyl acetate gave a yellow precipitate, which was separated by filtration and washed thoroughly with ethyl acetate to remove excess [Bu$_4$N]Cl. The solid was dissolved in CH$_2$Cl$_2$, reprecipitated with ethyl acetate, separated by filtration, washed successively with ethyl acetate and ether, and dried in vacuo. The yield of bright yellow-green solid was 0.32 g (58%). ^{31}P NMR (CD$_2$Cl$_2$) δ 67.8 [*J*(PtP) 2988 Hz]. Literature value for K$_4$[Pt$_2$(μ-pop)$_4$]: δ 66.1 [*J*(PtP) 3073 Hz].[10]

[PPN]$_4$[Pt$_2$(μ-pop)$_4$]. A solution of K$_4$[Pt$_2$(μ-pop)$_4$] (0.5 g, 0.43 mmol) in water (50 mL) was treated with [PPN]Cl (0.99 g, 1.73 mmol) in ethanol (50 mL). The initially yellow solution immediately became turbid, then clearer, and was stirred for 5 min. Addition of water (ca. 200 mL) precipitated the product, which was separated by filtration, washed successively with water and ether, and dried in vacuo. The yield of fluorescent yellow-green solid was quantitative (1.33 g). ^{31}P NMR (CD$_2$Cl$_2$) δ 67.7 [*J*(PtP) 3019 Hz].

[Bu$_4$N]$_4$[Pt$_2$(μ-pop)$_4$X$_2$] [X = Cl (2a), Br (2b), I (2c)]. To a solution of [Bu$_4$N]$_4$[Pt$_2$(μ-pop)$_4$] (0.15 g, 0.08 mmol) in CH$_2$Cl$_2$ (5 mL) was added dropwise about 1 equiv of X$_2$ [PhICl$_2$ (0.022 g, 0.08 mmol), Br$_2$ (5 μL, 0.1 mmol), or I$_2$ (0.023 g, 0.09 mmol)] dissolved in CH$_2$Cl$_2$ (3 mL). The color changed to dark yellow (X = Cl), orange (X = Br), or red-brown (X = I). The solution was stirred for 10 min, and the product was precipitated by dropwise addition of ether (15 mL). **2a**: bright yellow solid (0.15 g, 94%); **2b**: orange solid (0.13 g, 80%); **2c**: dark orange solid (0.15 g, 91%). Analytical and ^{31}P NMR data are collected in Table 2. The carbon analyses of the similarly prepared PPN$^+$ salts were consistently 2−5% low, possibly owing to incomplete combustion, and high chloride analyses on the PPN$^+$ salts of **1** (1.46%) and **2a** (3.93%; calcd 2.22%) suggested the presence of small amounts of chloride-containing impurities such as CH$_2$Cl$_2$.

Oxidation of [PPN]$_4$[Pt$_2$(μ-pop)$_4$] with [NO][BF$_4$]. Solid [NO][BF$_4$] (5 mg, 43 mmol) was added to a solution of [PPN]$_4$[Pt$_2$(μ-pop)$_4$] (132 mg, 43 mmol) in CH$_2$Cl$_2$ (10 mL). A dark solid precipitated, and the color of the solution changed from yellow to orange. After being stirred for 1 h, the slightly turbid solution was filtered though Celite into rapidly stirred ether (50 mL). The resulting precipitate was separated by filtration, washed with ether, and dried in vacuo to give 85 mg of an orange solid, **7a**, that showed a ν(NO) band at 1720 cm^{-1} in KBr or Nujol due to **8**. Attempts to purify the solid by fractional crystallization failed. A thin orange-yellow plate obtained by layering a CH$_2$Cl$_2$ solution with ether was selected for X-ray structural analysis and turned out to be **8** (see below).

Treatment of an orange solution of the isolated solid with an excess of [Bu$_4$N]X (X = Cl, Br, I) caused an immediate color change to yellow (X = Cl), pale orange (X = Br), and dark orange (X = I), and the ^{31}P NMR spectra now showed the characteristic peaks due to [Pt$_2$(μ-pop)$_4$X$_2$]$^{4-}$, together with peaks due to small amounts of unidentified side-products.

The elemental analysis of the initially formed dark solid was C 19.50; H 4.30; N 2.25; P 16.71; Cl 0.58%.

Oxidation of [Bu$_4$N]$_4$[Pt$_2$(μ-pop)$_4$] with [NO][BF$_4$]. Solid [NO][BF$_4$] (1.5 mg, 0.013 mmol) was added to a solution of [Bu$_4$N]$_4$[Pt$_2$(μ-pop)$_4$] (25 mg, 0.013 mmol). Work-up as described above gave an orange solid (14 mg) containing **7b** [ν(NO) (Nujol) 1720 cm^{-1}] and [Bu$_4$N][BF$_4$], which could not be separated. The ^{31}P NMR spectrum in CD$_2$Cl$_2$ showed no peaks but, on addition of an excess of [Bu$_4$N]Cl, the color changed from orange to yellow and the characteristic spectrum of [Pt$_2$(μ-pop)$_4$Cl$_2$]$^{4-}$ was observed, with almost no side-products.

Oxidation of [PPN]$_4$[Pt$_2$(μ-pop)$_4$] with AgBF$_4$. Solid AgBF$_4$ (4 mg, 0.02 mmol) was added to a yellow solution of [PPN]$_4$[Pt$_2$(μ-pop)$_4$] (64 mg, 0.02 mmol) in CH$_2$Cl$_2$ (10 mL), and the mixture was stirred in the dark for 30 min, during which time a dark orange precipitate formed. The solvent was stripped, and the crude solid used for IR studies.

X-ray Crystallography. The crystal of [PPN]$_3$[Pt$_2$(P$_2$O$_5$H$_2$)$_4$(NO)]·2Et$_2$O·CH$_2$Cl$_2$ (**8**) was mounted on a glass fiber in viscous paraffin oil at 123 K. A total of 74533 ($2\theta_{max}$ 50°) reflection data was obtained by use of a Bruker X8 APEX CCD diffractometer (Mo K$_\alpha$ radiation, λ 0.71073 Å) and the data were empirically corrected for absorption (SADABS).[62] The data were merged (R_{int} 0.075) to 20508 unique reflections, 14936 being considered "observed" [$I > 2\sigma(I)$]. The structure was solved by conventional methods and refined by full-matrix least-squares on all F^2 data using SHELX-97.[63] Anisotropic thermal parameter forms were refined for the Pt, Cl, and P atoms only. Hydrogen atoms on the PPN$^+$ cations were placed in calculated positions with C−H distances 0.95 Å and U_{iso}(H) = 1.2U_{eq}(C); hydrogen atoms on the [P$_2$O$_5$H$_2$]$^{2-}$ ligands could not be located but were placed on selected oxygen atoms in calculated positions with U_{iso}(H) = 1.2U_{eq}(O). This model matched that observed for the pop^{2-} anion in which the hydrogen atoms were located {e.g., K$_4$[Pt$_2$(pop)$_4$]·2H$_2$O,[2,8] K$_4$[Pt$_2$(pop)$_4$I$_2$]·2H$_2$O[11]}. The oxygen atom O(21) of the NO ligand was modeled as disordered over two positions with occupancies fixed at 0.60:0.40 after trial refinement, and the N−O distances were restrained to be equal.

C$_{117}$H$_{120}$Cl$_2$N$_4$O$_{23}$P$_{14}$Pt$_2$: FW 2844.83. Triclinic, $P\bar{1}$. a = 14.4911(4), b = 16.5138(4), c = 24.8553(7) Å. α = 90.581(1), β = 94.069(1), γ = 92.801°. V = 5925.3(3) Å^3. Z = 2, d_{calc} = 1.594 g.cm^{-1}. μ = 2.665 mm^{-1}. Crystal size 0.20 × 0.18 × 0.02 mm. θ range 1.93−25.00°. T_{min}/T_{max} 0.95, 0.62. Data/restraints/param. 20508/4/746. GOF 1.138. $R1$ [$I > 2\sigma(I)$] 0.082. wR^2 (all data) 0.168. Residual electron density 1.86, −3.34 e Å^{-3}; the highest peak is located 0.92 Å from Pt(2).

Acknowledgment. We thank Professor Keith Murray and Dr. Boujemaa Moubaraki at Monash University for magnetic

measurements, and Dr. John Boas at Monash University for EPR measurements at liquid helium temperature on **7a**.

Supporting Information Available: X-ray crystallographic data in CIF format for complex **8**, Figure S1 showing cyclic voltammograms of $[Pt_2(\mu\text{-pop})_4]^{4-}$ in CH_2Cl_2 as a function of scan rate for the first oxidation process at a glassy carbon electrode at −75 °C and Figure S2 showing cyclic voltammograms and UV−visible spectra of an equimolar mixture of $[Pt_2(\mu\text{-pop})_4Br_2]^{4-}$ and $[Pt_2(\mu\text{-pop})_4Br_2]^{4-}$. This material is available free of charge via the Internet at http://pubs.acs.org.

IC802213V

(62) Sheldrick, G. M. *SADABS*; University of Göttingen: Göttingen, Germany, 1996 (part of the *Bruker Apex 2* v 2.0 program system, Bruker AXS, Madison, WI, 2005).

(63) Sheldrick, G. M. *SHELX-97*; University of Göttingen: Göttingen, Germany, 1997.